An exact relation between Eulerian and Lagrangian velocity increment statistics

O. Kamps,[1] R. Friedrich,[1] and R. Grauer[2]

[1] *Theoretische Physik, Universität Münster, Germany*
[2] *Theoretische Physik I, Ruhr-Universität Bochum, Germany*

(Dated: October 1, 2008)

We present a formal connection between Lagrangian and Eulerian velocity increment distributions which is applicable to a wide range of turbulent systems ranging from turbulence in incompressible fluids to magnetohydrodynamic turbulence. For the case of the inverse cascade regime of two-dimensional turbulence we numerically estimate the transition probabilities involved in this connection. In this context we are able to directly identify the processes leading to strongly non-Gaussian statistics for the Lagrangian velocity increments.

PACS numbers: 47.10.ad,47.27.-i,47.27.E-,02.50.Fz

arXiv:0809.4339v2 [physics.flu-dyn] 1 Oct 2008

Introduction The relation between Eulerian and Lagrangian statistical quantities is a fundamental question in turbulence research. It is of crucial interest for the understanding and modeling of transport and mixing processes in a broad range of research fields spanning from cloud formation in atmospheric physics over the dispersion of microorganisms in oceans to research on combustion processes and the understanding of heat transport in fusion plasmas. The recent possibility to assess the statistics of Lagrangian velocity increments by experimental means [1, 2] has stimulated investigations of relations between the Eulerian and the Lagrangian two-point velocity statistics. Especially, the emergence of intermittency (i.e. the anomalous scaling of the moments of the velocity increment distributions [3]) in both descriptions and its interrelationship is of great importance for our understanding of the spatio-temporal patterns underlying turbulence. A first attempt to relate Eulerian and Lagrangian statistics has been undertaken by Corrsin [4], who investigated Eulerian and Lagrangian velocity correlation functions. Recently, the Corrsin approximation has been reconsidered by [5], where it has become evident that it is a too crude approximation and cannot deal with the question of the connection between Eulerian and Lagrangian intermittency. Further approaches to characterize Lagrangian velocity increment statistics are based on multifractal models [6, 7] which also have been extended to the dissipation range [8]. In [7] a direct translation of the Eulerian multifractal statistics to the Lagrangian picture is presented. In this approach a non-intermittent Eulerian velocity field cannot lead to Lagrangian intermittency. This statement is in contrast with the experimental results of Rivera [9], as well as numerical calculations performed for 2d turbulence [10]. Motivated by this fact we have derived an exact relation between the Eulerian and the Lagrangian velocity increment distributions, which allows to study the emergence of Lagrangian intermittency from a statistical point of view.

Connecting the increment PDFs The quantities of interest are the Eulerian velocity increments

$$u_e = v(\boldsymbol{y}+\boldsymbol{x},t) - v(\boldsymbol{y},t), \tag{1}$$

where the velocity difference is measured at the time t between two points that are separated by the distance $\boldsymbol{x}$, and the Lagrangian velocity increment

$$u_l = v(\boldsymbol{y}+\tilde{\boldsymbol{x}}(\boldsymbol{y},\tau,t),t) - v(\boldsymbol{y},t-\tau). \tag{2}$$

In the latter case the velocity difference is measured between two points connected by the distance $\tilde{\boldsymbol{x}}(\boldsymbol{y},\tau,t)$ traveled by a tracer particle during the time interval τ. In both cases v is defined as the projection $\boldsymbol{v}\cdot\hat{\boldsymbol{e}}_i$ of the velocity vector on one of the axes ($i = x, y, z$ in 3d and $i = x, y$ in 2d) of the coordinate system (see e.g. [12, 13]). In the case of an isotropic flow the results do not depend on the chosen axis, however we do not have to make this assumption yet. Additionally, we define the velocity increment

$$u_{el} = v(\boldsymbol{y}+\tilde{\boldsymbol{x}}(\boldsymbol{y},\tau,t),t) - v(\boldsymbol{y},t), \tag{3}$$

which is a mixed Eulerian-Lagrangian quantity because the points are separated by $\tilde{\boldsymbol{x}}$ but the velocities are measured at the same time. The properties of this quantity have been investigated in [14]. Finally, we introduce

$$u_p = v(\boldsymbol{y},t) - v(\boldsymbol{y},t-\tau), \tag{4}$$

measuring the velocity difference over the time τ at the starting point of the tracer. Following [15, 16] we define the so called fine-grained PDF for u_e as

$$\hat{f}_e(v_e;\boldsymbol{x},\boldsymbol{y},t) = \delta(u_e - v_e). \tag{5}$$

where u_e is the random variable and v_e is the independent sample-space variable. The fine-grained PDF describes the elementary event of finding the value v_e given the measured $u_e = v(\boldsymbol{y}+\boldsymbol{x},t) - v(\boldsymbol{y},t)$. The relation to the PDF is determined by

$$f_e(v_e;\boldsymbol{x},\boldsymbol{y},t) = \langle \hat{f}_e(v_e;\boldsymbol{x},\boldsymbol{y},t)\rangle, \tag{6}$$

where the brackets denote ensemble averaging. The quantity f_e is a function with respect to the variables $\boldsymbol{x}, \boldsymbol{y}, t$ and a PDF with respect to the variable v_e. In analogy to (5) we can define fine-grained PDFs for all other quantities. Now we want to derive an exact relation between the fine-grained PDFs $\hat{f}_e$ and $\hat{f}_l$. This task can be split up into two steps. First we have to replace the distance $\boldsymbol{x}$ by the trajectory $\tilde{\boldsymbol{x}}(\boldsymbol{y}, \tau, t)$ of a tracer in order to translate from u_e to u_{el}. This is done by

$$\hat{f}_{el}(v_e;\boldsymbol{y}, \tau, t) = \int d\boldsymbol{x}\ \delta(\tilde{\boldsymbol{x}}(\boldsymbol{y}, \tau, t) - \boldsymbol{x}) \hat{f}_e(v_e; \boldsymbol{x}, \boldsymbol{y}, t). \quad (7)$$

We see that during this operation the sample-space variable is not affected. The subscript in $\hat{f}_{el}$ denotes the fact that we now have $v_e = u_{el}$ instead of $v_e = u_e$. In the second step we have to connect $\hat{f}_l$ and $\hat{f}_{el}$. From the definitions of the increments (2) - (4) we see that $u_l = u_{el} + u_p$ and therefore the fine-grained PDF for u_l is given by the fine-grained distribution of the sum of u_{el} and u_p. To that end we have to multiply $\hat{f}_{el}(v_e; \boldsymbol{y}, \tau, t)$ with $\hat{f}_{el}(v_e; \boldsymbol{y}, \tau, t) = \delta(u_p - v_p)$ to get the fine-grained joint probability of finding u_{el} and u_p at the same time. Subsequent application of $\int dv_e \int dv_p\ \delta(v_l - (v_e + v_p))$ leads to

$$\hat{f}_l(v_l; \boldsymbol{y}, \tau, t) = \int dv_e\ \hat{f}_p(v_l - v_e; \boldsymbol{y}, \tau, t) \hat{f}_{el}(v_e; \boldsymbol{y}, \tau, t). \quad (8)$$

To derive the corresponding PDFs we have to perform the ensemble average. In case of equation (8) we obtain

$$\begin{aligned} f_l(v_l; \boldsymbol{y}, \tau, t) &= \left\langle \int dv_e\ \hat{f}_p(v_l - v_e; \boldsymbol{y}, \tau, t) \hat{f}_{el}(v_e; \boldsymbol{y}, \tau, t) \right\rangle \\ &= \int dv_e\ f_p(v_l - v_e | v_e; \boldsymbol{y}, \tau, t) f_{el}(v_e; \boldsymbol{y}, \tau, t). \end{aligned} \quad (9)$$

In the last line we used the general relation $p(a, b) = p(a|b)p(b)$ valid for two random variables in order to extract f_{el} from the average. We can treat (7) in a similar manner. This leads us to

$$\begin{aligned} f_{el}(v_e; \boldsymbol{y}, \tau, t) &= \left\langle \int d\boldsymbol{x}\ \delta(\tilde{\boldsymbol{x}}(\boldsymbol{y}, \tau, t) - \boldsymbol{x}) \hat{f}_e(v_e; \boldsymbol{x}, \boldsymbol{y}, t) \right\rangle \\ &= \int d\boldsymbol{x}\ \langle \delta(\tilde{\boldsymbol{x}}(\boldsymbol{y}, \tau, t) - \boldsymbol{x}) | v_e \rangle \hat{f}_e(v_e; \boldsymbol{x}, \boldsymbol{y}, t). \end{aligned} \quad (10)$$

Inserting equation (9) into (10) shows that the Eulerian and the Lagrangian velocity increment PDFs are connected via the transition probabilities $p_a = \langle \delta(\tilde{\boldsymbol{x}}(\boldsymbol{y}, \tau, t) - \boldsymbol{x}) | v_e \rangle$ and $p_b = f_p(v_l - v_e | v_e; \boldsymbol{y}, \tau, t) = f_p(v_p | v_e; \boldsymbol{y}, \tau, t)$.

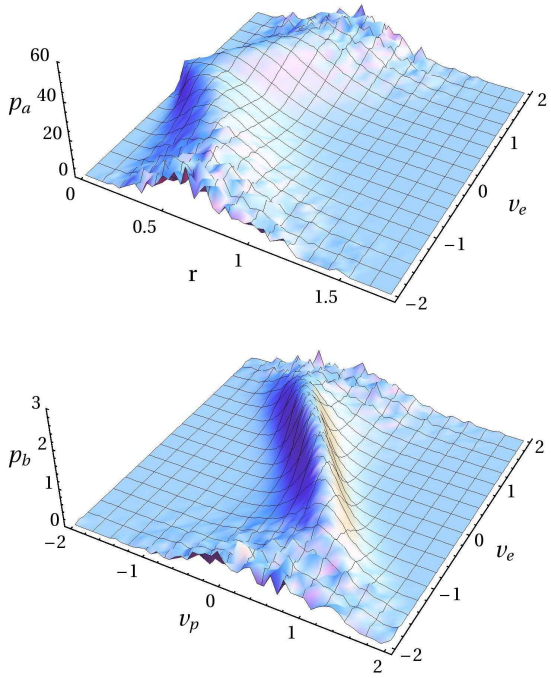

FIG. 1: The plot shows $p_a(r|v_e;\tau)$ (top) and $p_a(v_p|v_e;\tau)$ (bottom) for $\tau = 0.09T_I$.

Before we connect both equations we introduce some simplifications. In most experiments and numerical simulations dealing with Lagrangian statistics the flow is assumed to be stationary and homogeneous. In this case we may average with respect to $\boldsymbol{y}$ and t and hence the dependence on this parameters in (10) and (9) drops. Under the assumption of isotropy f_{el} depends only on $r = |\boldsymbol{x}|$. Therefore, we can introduce spherical coordinates in (10) and integrate with respect to the angles. As mentioned before, in the case of isotropy the statistical quantities do not depend on the chosen axis. Finally we arrive at

$$f_l(v_l;\tau) = \int dv_e p_b(v_l - v_e | v_e;\tau) \underbrace{\int_0^\infty dr\ p_a(r|v_e;\tau)\ f_e(v_e;r)}_{f_{el}(v_e;\tau)}. \quad (11)$$

For convenience, we included the integrated functional determinant ($2\pi r$ in two and $4\pi r^2$ in three dimensions) in p_a. In this case $p_a(r|v_e;\tau)$ is a measure for the turbulent transport and gives the probability of finding a tracer traveling the absolute distance r within the time interval τ. Multiplication by $f_e(v_e;r)$ and subsequent integration over the whole r-range mixes the Eulerian statistics from different length scales r weighted by p_a to form the PDF $f_{el}(v_e;\tau)$ for a fixed time-delay τ. The occurence of the condition in p_a shows that this weighting depends on u_e. changes by u_p. The transition probability p_b incorporates

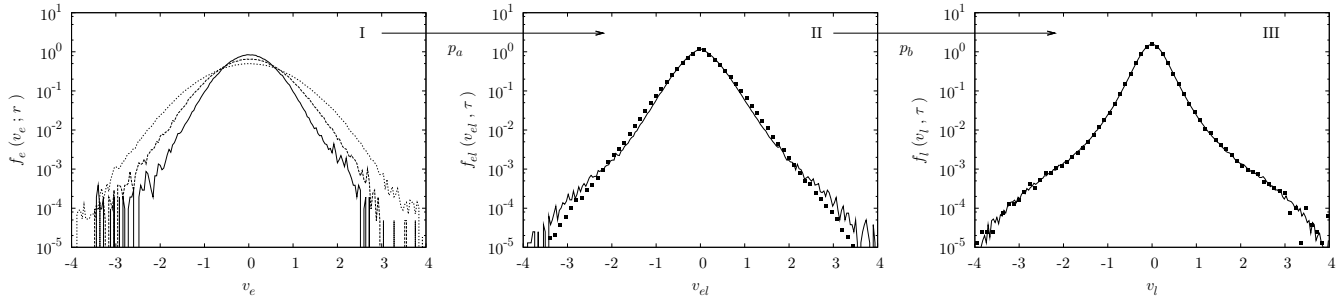

FIG. 2: The figure shows the impact of the transition probabilities on the Eulerian PDF. The left part of the figure shows $f_e(v_e;r)$ for $r = 0.06, 0.12, 0.3$. These PDFs are transformed into $f(v_e;\tau)$ (middle) by the transition PDF presented in the upper half of Fig. 1. Subsequently $f(v_e;\tau)$ is converted into $f_l(v_l;\tau)$ (right picture) by the second transition PDF from Fig. 1. In both cases $\tau = 0.09T_I$. In plot II and III the points denote the reconstructed PDFs based on (10) and (9) and the lines denote the PDFs directly computed from the Lagrangian data.

the fact that during the motion of the tracer particle the velocity at the starting point Multiplying $f_{el}(v_e;\tau)$ with p_b and integrating over v_e sorts all events where $u_{el}+u_p = u_l$ into the corresponding bin of the histogram for u_l. We want to stress that equations (10) and (9) and except from symmetry considerations also equation (11) are of a purely statistical nature and, as a consequence, hold for quite different turbulent fields. They are valid for two-dimensional as well as three-dimensional incompressible turbulence but can also be applied to magnetohydrodynamic turbulence. The differences in the details of these turbulent systems, which are connected to the presence of different types of coherent structures like localized vortices in the case of incompressible fluid turbulence or sheet-like structures in magnetohydrodynamic turbulence, are therefore closely related to the functional form of p_a and p_b.

Two-dimensional turbulence In this section we want to estimate numerically the two transition PDFs in (11) for the case of the inverse energy cascade of two-dimensional turbulence. The data are taken from a pseudospectral simulation of the inverse energy cascade in a periodic box with box-length 2π [10]. Recapitulating the derivation of (11) we see that we need the velocity at the start and the end point of a tracer trajectory at the same time to estimate the transition PDFs. Therefore we have to record the velocity at the starting points of the tracers additionally to their current position and their current velocity. In Fig. 1 the transition probabilities p_a and p_b are depicted for $\tau = 0.09T_I$, where T_I denotes the Lagrangian integral time scale [11]. We have chosen this rather small time lag as an example because in this case the deviation of the Lagrangian increment PDF from a Gaussian is significant. The transition probability p_a can be approximated by

$$p_a(r|v_e;\tau) = N(v_e,\tau) r \exp[-(r - m(v_e,\tau))^2/\sigma^2(v_e,\tau)]. \tag{12}$$

For small v_e we have $m(v_e,\tau) \sim \alpha(\tau)|v_e|$ and $\sigma^2(v_e,\tau)) \sim \beta(\tau)$. From the functional form of p_a one can see that the transport of the tracer particles is of probabilistic nature. For any fixed v_e the tracers travel different distances during the same time τ. We also see a strong dependence on the condition v_e which can be interpreted as deterministic part of the turbulent transport. This distinguishes it from pure diffusion and directly shows that the widely used Corrsin approximation is violated. In the case of deterministic transport p_a would be proportinal to $\delta(r - m(v_e,\tau))$. A good approximation for p_b is given by

$$p_b(v_p|v_e;\tau) = N(v_e,\tau)\exp[-(u_p - m(v_e,\tau))^2/\sigma^2(v_e,\tau)] \tag{13}$$

with $m(v_e,\tau) = \alpha(\tau)\tanh(\beta(\tau)v_e)$ and $\sigma^2(v_e,\tau) = \gamma(\tau)(1+\delta(\tau)|v_e|)$. For small v_e we see a strong negative correlation between v_e and v_p (here $\tanh(v_e) \sim v_e$). Both quantities tend to cancel in this case. This negative correlation between the sample-space variables in p_b is connected with the sweeping effect. For a tracer starting with v_1 travelling the time τ without changing its velocity we have $u_{el} = v_1 - v_2$ when the velocity at the starting point changes during τ from v_1 to v_2. In this case we have $u_p = v_2 - v_1 = -u_{el}$. This corresponds to an idealized situation but it gives a hint at the cause of the negative correlations in p_b. For larger v_e the correlation decreases. This is captured by the fact that $\tanh(\beta(\tau)v_e) \sim const$ for large v_e. For both transition PDFs we observe that for increasing τ the dependence on their conditions vanishes.

Now we want to turn to the question how the transition PDFs transform the Eulerian PDF $f_e(v_e;r)$ into the Lagrangian PDF $f_l(u_l;\tau)$. This process is depicted in Fig. 2. The left part of the figure shows several examples of $f_e(v_e;r)$. Applying $\int dr\ p_a(r|v_e;\tau)$ (see equation 11) superposes different Eulerian PDFs $f_e(v_e;r)$ with different variances leading to the triangular shape in the semilogarithmic plot of the new PDF $f_{el}(v_e;\tau)$ (middle of Fig.2). During the transition from $f_{el}(v_e;\tau)$ to $f_l(v_l;\tau)$

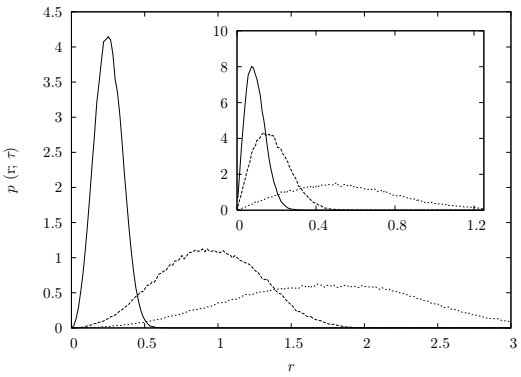

FIG. 3: The figure shows $p_a(r;\tau)$ for $\tau = 3.5\tau_\eta,\ 14\tau_\eta,\ 28\tau_\eta$ for three-dimensional turbulence. In the inset p_a is depicted for the two-dimensional case with $\tau = 0.22T_I, 0.44T_I, 0.9T_I$

the variables v_p and v_e are added to form v_l. The previously described observation that v_p and v_e tend to cancel each other for small v_e leads to a stronger weighting of very small v_l so that the new PDF $f_l(v_l;\tau)$ is strongly peaked around zero (right part of Fig.2). In contrast to the center of the distribution the tails seem not to be influenced significantly by $p_b(v_p|v_e;\tau)$. This is in agreement with the fact that for large v_e the correlation between v_e and v_l decreases.

Three-dimensional turbulence To get an impression of the transition probabilities in three dimensional turbulence we used the data provided by [7, 17] to calculate the PDF $p_a(r;\tau) = \int dv_e\ p_a(r|v_e;\tau)$ for different τ. The result is depicted in Fig. 3. We see that as in the two-dimensional case the Lagrangian time scale τ is related to the Eulerian length scales by a PDF. This well known result shows that in principle it is not possible to connect them by a Kolmogorov type relation like $\tau \sim r/\delta u_r$ [7]. In this relation τ is a typical eddy turnover time connected to eddies of length scale r. In our example we have chosen three different values of the time delay τ taken from the inertial range. Even when the maximum of p_a is at a distance r which lies in the Eulerian inertial range there are significant contributions from very small and very large r. From this observation we can conclude that due to the turbulent transport the Lagrangian statistics is influenced by contributions from the Eulerian integral and dissipative length scales.

Relation to the Multifractal approach The characterization of the relation between Eulerian and Lagrangian PDFs with the help of the conditional probabilities $p_a(r|v_e;\tau)$ (Eulerian to semi-Lagrangian transition) and $p_b(v_p|v_e;\tau)$ (semi-Lagrangian to Lagrangian transition) allows one to recover a well known multifractal approach for relating Eulerian and Lagrangian structure function exponents [7]. As a side product, a simpler formula for the Lagrangian structure function exponents of this multifractal approach will be obtained. Regarding the translation rule in [7] we would have a fixed relationship $|\tilde{\boldsymbol{x}}| \sim v_e\tau$ (δu_r corresponds to u_e in our notation) between the time lag τ and the distance traveled by a tracer particle during this time. This would correspond to choosing $p_a \sim \delta(r - v_e\tau)$ in (11). The additional assumption [7] $\delta v_\tau \sim \delta u_r$ ($u_l \sim u_e$ in our notation) that the velocity fluctuations on the time scale τ are proportional to the fluctuations on the length scale r could be incorporated in our framework by choosing $p_b \sim \delta(v_l - v_e)$ leading to

$$\begin{aligned} f_l(v_l;\tau) &= \int dv_e\, \delta(v_l - v_e) \int_0^\infty dr\, \delta(r - v_e\tau) f_e(v_e;r) \\ &= f_e(v_l; v_l\tau). \end{aligned} \tag{14}$$

The exponents for the Lagrangian structure function exponents can now be obtained by making use of the Mellin transform

$$f_e(v_e, r) = \frac{1}{v_e} \int_{-i\infty}^{i\infty} dn\, S_e(n) v_e^{-n} \tag{15}$$

with $S_e(n) = A_e(n) r^{\zeta_e(n)}$. Here, we use the same notation as in [18]. Please note, that it will be not neccessary to know the amplitudes $A_e(n)$ but only the Eulerian scaling exponents $\zeta_e(n)$. Using Eqn. (14) and the Mellin transform we obtain

$$f_l(v_l;\tau) = \frac{1}{v_l} \int_{-i\infty}^{i\infty} dn\, A_e(n) \tau^{\zeta_e(n)} v_l^{\zeta_e(n)-n}. \tag{16}$$

This Lagrangian PDF is now inserted into the inverse Mellin transform to obtain the Lagrangian structure functions

$$\begin{aligned} S_l(n) &= \int_0^\infty dv_l\, v_l^n f_l(v_l;\tau) \\ &= \int_0^\infty dv_l\, \frac{1}{v_l} v_l^n \int_{-i\infty}^{i\infty} dj\, A_e(j) \tau^{\zeta_e(j)} v_l^{\zeta_e(j)-j}. \end{aligned} \tag{17}$$

Now we substitute $j'(j) = j - \zeta_e(j)$, $dj' = (1 - \partial_j\zeta_e(j))dj$ and denote the inverse function by $j = j(j')$. Thus we have

$$S_l(n) = \int_0^\infty dv_l\, \frac{1}{\delta v_l} v_l^n \int_{-i\infty}^{i\infty} dj'\, S_l(j') (\delta v_l)^{-j'} \tag{18}$$

with $S_l(j') = \frac{A_e(j)}{1-\partial_j\zeta_e(j)} \tau^{\zeta_e(j)}$ and $j' = j - \zeta_e(j)$ and we obtain for the exponents

$$\zeta_l(n - \zeta_E(n)) = \zeta_e(n) \tag{19}$$

It remains to show that this relation (19) is identical to the formulas derived in Biferale *et al.* [7]. To see this, we shortly repeat the multrifractal approach which starts with the Eulerian structure function exponents

$$\zeta_e(p) = \inf_h (ph + 3 - D_e(h)) = ph_e^* + 3 - D_e(h_e^*) \tag{20}$$

and $p = D'_e(h^*_e)$. Here $D_e(h)$ is the Eulerian singularity spectrum and h^*_e is the value where the infimum is achieved. The assumption $r = v_e\tau$ appears now in the denominator of the expression of the Lagrangian structure function exponents

$$\zeta_l(p) = \inf_h \left(\frac{ph + 3 - D_e(h)}{1-h} \right). \quad (21)$$

From this it follows

$$\zeta_l(p - \zeta_e(p)) = \inf_h \left(\frac{(p - ph^*_e - 3 + D_e(h^*_e))h + 3 - D_e(h)}{1-h} \right). \quad (22)$$

In order to find the infimum we differentiate with respect to h

$$D'_e(h^*_e) - D'_e(h) + D_e(h^*_e) - D_e(h) - D'_e(h^*_e)h^*_e + D'_e(h)h \stackrel{!}{=} 0 \quad (23)$$

From this it follows that $h^*_L = h^*_E$ and

$$\zeta_L(p - \zeta_e(p)) = ph^*_e + 3 - D_e(h^*_e) = \zeta_e(p) \quad (24)$$

which recovers (19). A consequence of (19) and (14) is that for a self-similar Eulerian velocity field (as we can find it in the two dimensional inverse energy cascade) we should find self similar Lagrangian PDFs. As mentioned above this is in contradiction to recent experiments [9] and our own numerical simulations [10].

Conclusion and Outlook We presented a straight forward derivation of an exact relationship between Eulerian and Lagrangian velocity increment PDFs. For the example of two-dimensional forced turbulence we were able to explain how it is possible to observe strongly non-Gaussian intermittent distributions for the Lagrangian velocity increments. The two mechanisms in this context are the turbulent transport of the tracers leading to the mixing of statistics from different length scales and the velocity change at the starting point of the tracers leading to a further deformation of the increment PDF. In comparison we analyzed data from simulations of three- dimensional turbulence. Similar to the two-dimensional case we demonstrated that Lagrangian time- and Eulerian length-scales are connected via a transition PDF that varies with the time scale. We where also able to show that the well known multifractal model for the Lagrangian structure functions ia a limiting case of the presented translation rule. The next step is to estimate the transition probabilities for three-dimensional turbulence as well as magnetohydrodynamic turbulence in order to get a deeper understanding of the influence of the underlying physical mechanisms, especially the presence of coherent structures on the translation process. In this context the question why intermittency in the Lagrangian picture is stronger in magnetohydrodynamics than in fluid turbulence [19], although the situation is reversed in the Eulerian picture, will be addressed.

Acknowledgements We are grateful to H. Homann, M. Wilczek and D. Kleinhans for fruitful discussions and acknowledge support from the Deutsche Forschungsgesellschaft (FR 1003/8-1, FG 1048). We also thank the supercomputing center Cineca (Bologna, Italy) for providing and hosting of the data for 3D Turbulence.

[1] A. La Porta, G. Voth, A.M. Crawford, J. Alexander, and E. Bodenschatz, Nature **409**, 1017 (2001).
[2] N. Mordant, P. Metz, O. Michel and J.-F. Pinton, Phys. Rev. Lett. **87**, 214501 (2001).
[3] U. Frisch, Cambridge University Press, (1995)
[4] S. Corrsin, Advances in Geophysics, Vol. 6, ed. F.N. Freinkel and P.A. Sheppard (New York Academic), pp 161 (1959).
[5] S. Ott and J. Mann, J. Fluid Mech. **422**, 207 (2000).
[6] M. S. Borgas, Philos. Trans. R. Soc. London, Ser. A **342**, 379 (1993)
[7] L. Biferale, G. Bofetta, A. Celani, B.J. Devinish, A. Lanotte, and F. Toschi, Phys. Rev. Lett. **93**, 064502 (2004).
[8] L. Chevillard, S.G. Roux, E. Lévêque, N. Mordant, J.-F. Pinton, A. Arneodo, Phys. Rev. Lett. **91**, 214502 (2003)
[9] M. K. Rivera and R. E. Ecke, arXiv.org:0710.5888, (2007).
[10] O. Kamps and R. Friedrich, Phys. Rev. E **78**, 036321 (2008).
[11] P. K. Yeung, Annual Review of Fluid Mechanics, 34, (2002).
[12] N. Mordant, E. Lévêque and J.-F. Pinton, New. Journ. Phys. **6** , 116 (2004).
[13] G. Voth, A. L. Porta, A. Crawford, J. Alexander, E. Bodenschatz, Journal of Fluid Mechanics, (2002).
[14] R. Friedrich, R. Grauer, H. Homann, O. Kamps, arXiv:0705.3132v1, (2007).
[15] T. S. Lundgren, Phys. Fluids **10**, 969 (1967).
[16] S. B. Pope, Cambridge University Press, (2000).
[17] L. Biferale, G. Boffetta, A. Celani, A. Lanotte, and F. Toschi, Phys. Fluids **17**, 021701 (2005).
[18] V. Yakhot, Physica D **215**, 166 (2006).
[19] H. Homann, R. Grauer, A. Busse, and W.C. Müller, J. Plasma Phys. **73**, 821 (2007).